

In-situ etch-depth control better than 5 nm with reflectance anisotropy spectroscopy (RAS) equipment during reactive ion etching (RIE): A technical RAS application

Cite as: AIP Advances 9, 075116 (2019); <https://doi.org/10.1063/1.5099526>

Submitted: 11 April 2019 . Accepted: 12 July 2019 . Published Online: 22 July 2019

Christoph Doering, Johannes Strassner, and Henning Fouckhardt



View Online



Export Citation



CrossMark

AVS Quantum Science

Co-published with AIP Publishing



Coming Soon!

In-situ etch-depth control better than 5 nm with reflectance anisotropy spectroscopy (RAS) equipment during reactive ion etching (RIE): A technical RAS application

Cite as: AIP Advances 9, 075116 (2019); doi: 10.1063/1.5099526

Submitted: 11 April 2019 • Accepted: 12 July 2019 •

Published Online: 22 July 2019



View Online



Export Citation



CrossMark

Christoph Doering,^{a)} Johannes Strassner, and Henning Fouckhardt

AFFILIATIONS

Integrated Optoelectronics and Microoptics Research Group, Physics Department, Technische Universität Kaiserslautern (TUK), PO Box 3049, D-67653 Kaiserslautern, Germany

^{a)}Electronic mail: cdoering@physik.uni-kl.de

ABSTRACT

A measurement technique, i.e. reflectance anisotropy/difference spectroscopy (RAS/RDS), which had originally been developed for in-situ epitaxial growth control, is employed here for in-situ real-time etch-depth control during reactive ion etching (RIE) of cubic crystalline III/V semiconductor samples. Temporal optical Fabry-Perot oscillations of the genuine RAS signal (or of the average reflectivity) during etching due to the ever shrinking layer thicknesses are used to monitor the current etch depth. This way the achievable in-situ etch-depth resolution has been around 15 nm. To improve etch-depth control even further, i.e. down to below 5 nm, we now use the optical equivalent of a mechanical vernier scale— by employing Fabry-Perot oscillations at two different wavelengths or photon energies of the RAS measurement light – 5% apart, which gives a vernier scale resolution of 5%. For the AlGaAs(Sb) material system a 5 nm resolution is an improvement by a factor of 3 and amounts to a precision in in-situ etch-depth control of around 8 lattice constants.

© 2019 Author(s). All article content, except where otherwise noted, is licensed under a Creative Commons Attribution (CC BY) license (<http://creativecommons.org/licenses/by/4.0/>). <https://doi.org/10.1063/1.5099526>

I. INTRODUCTION

Dry-etch-depth control is an important issue in crystalline semiconductor technology, since either device yield is low for etching too deep or process time is drastically increased for etching too shallow, because in the latter case the wafers would have to be etched again. Moreover, the etching can be hampered by statistically occurring etch interruptions due to unintentional sputter deposition of material from the vacuum chamber wall or from the sample holder. Therefore, precise in-situ and real-time etch-depth control would be highly appreciated.

Reflectance anisotropy/difference spectroscopy (RAS/RDS) had originally been developed as a means for epitaxial growth control, see e.g. Refs. 1–4. It is an accepted tool to monitor layer thickness, composition, doping, occurrence of quantum dots, and more.^{1–5} A very good review on RAS can be found in Ref. 6. In Ref. 7 even the use of RAS for the measurement of the optical

properties of graphene nanoribbons is reported. In Ref. 8 the innovative application of RAS to gas sensing is explained.

Since spectral RAS signal peaks are sometimes related to orderly oriented electric dipoles at the crystalline surface (especially for crystalline III/V semiconductors due to their ionic bond share), the attempt suggests itself to use RAS also for monitoring the etch depth during reactive ion etching (RIE) of crystalline material (in our case AlGaAs(Sb)). Successful trials to do so have been reported by us earlier.^{9–11}

Standard in-situ real-time resolution in such etch-depth control has been around 15 nm, while it might even be forced down to just a few lattice constants, as we will show in this contribution by use of an optical Vernier scale.

Moreover, application of RAS during RIE (RIE-RAS) also allows to perceive etch delays and interruptions and as a consequence it allows to correct the total etch-time on the fly. This way device yield should be drastically increasable with RIE-RAS.

II. EXPERIMENTAL

A. RAS principle

In Fig. 1 the principle of a RAS measurement is illustrated. The RAS equipment incorporates a broad-band light source, like a Xe lamp. The emitted originally non-polarized light wave is linearly polarized by a polarizer. Then the now polarized light wave enters the vacuum chamber through a viewport and impinges onto the sample perpendicularly to the surface.

The linearly polarized light wave can be understood as composed of two linearly polarized wave parts with orthogonal linear polarization. In case of cubic crystals: whenever the orientation of a plane of polarization of one wave part coincides with a main crystal axis, the orientation of the plane of polarization of the other wave part will coincide with another main crystal axis.

For the hypothetical case of a perfectly flat and ideal surface, normal incidence should not give any difference in reflectance for the two wave parts (in this case it is not even possible to define planes of polarization, because a plane of incidence does not exist for normal incidence). But anisotropies (like for instance the already mentioned orderly arranged electric dipoles at the surface) and certain surface reconstructions break the symmetry and a difference in the reflectivity for the two wave parts will occur and can be retrieved from the measurement.

The genuine RAS signal is defined as:

$$\frac{\Delta R}{R} = \frac{R_{[-110]} - R_{[110]}}{\langle R \rangle} \quad (1)$$

with the symbol R for reflectivities/reflectances and taking the main crystal axes $[-110]$ and $[110]$ exemplarily here. $\langle R \rangle$ is the average of the reflectivities for both wave parts. Typical signal heights are on the order of 10^{-3} , but the measurement technique is even sensitive down to 10^{-5} .

In general due to the reflectance difference the overall reflected wave is altered from linearly to slightly elliptically polarized. In order to detect the RAS signal and the state of polarization (the ellipticity) of the reflected wave, it is detected with a photoelastic modular

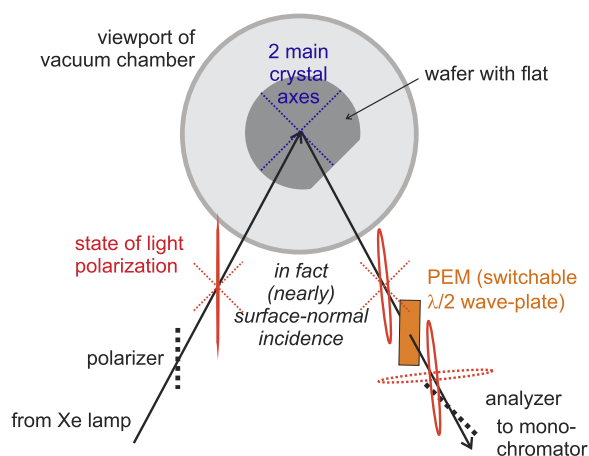


FIG. 1. Illustration of the RAS measurement principle. PEM = photoelastic modulator, operated at 50 kHz modulation frequency. On the contrary to the drawing the real angle of light incidence onto the wafer surface is nearly zero.

(PEM) as a switchable half-wave plate in combination with a second polarizer (i.e. an analyzer), a monochromator, and a detector. The PEM together with the analyzer allows for periodical detection of both wave parts.

RAS signals and spectral peaks are reproducible and their origins are understood; but their magnitude and shape are hard to calculate quantitatively (see e.g. Refs. 6 and 12).

During epitaxy the wafer is usually rotated with 1/s, so that there are only certain angular windows of the sample orientation (occurring periodically and twice per cycle), when/where the reflectances can be measured. On the contrary for etching wafer rotation is not necessary and the sample is just aligned angularly once for signal maximization before the beginning of the etch process.

B. RAS implementation in RIE system (vacuum chamber preparation)

In order to combine RIE with RAS the used parallel plate etch reactor had to be modified to provide for optical access from the RAS system outside the chamber to the wafer of interest inside. Therefore only two essential changes of the plasma reactor are necessary: we introduced a hole in the upper electrode/plate and - above this hole - an optical viewport in the vacuum chamber. Figure 2 contains a photograph of our RIE parallel plate reactor (by Roth & Rau,

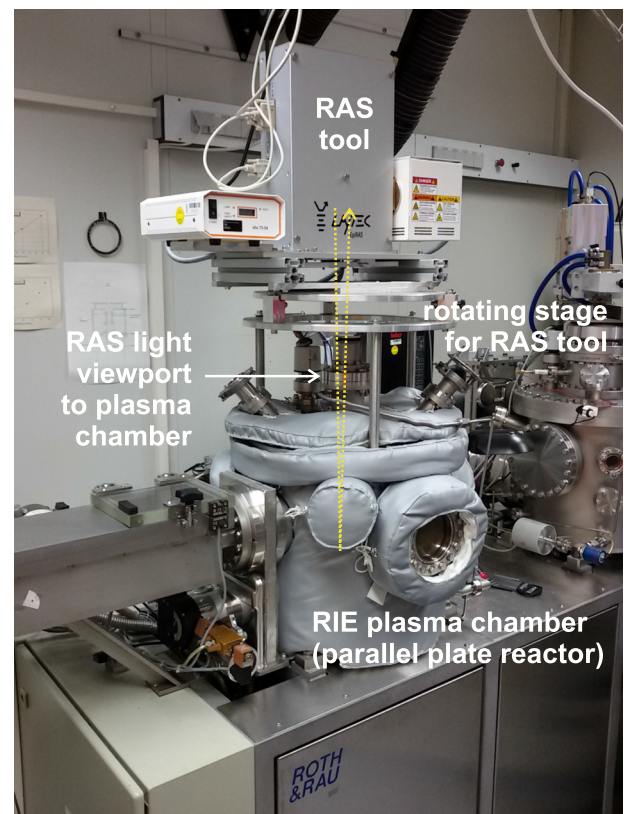


FIG. 2. Photograph of the parallel plate reactor RIE system MicroSys 350 by Roth & Rau, Wuestenbrand, Germany with the RAS system EpiRAS by Laytec, Berlin, Germany on top.

Wuestenbrand, Germany) with the RAS apparatus *EpiRas*[®] *TT* (by Laytec, Berlin, Germany¹³) on top. Detailed setup configurations can be found in Ref. 9.

The RAS system has to be aligned (just once before etching) in order to give best possible alignment of the plane of polarization with the 45° diagonal between two main crystal axes of the cubic material and hence to maximize the RAS signal. Therefore, the rack for the RAS system has to be rotatable around the vertical axis of the vacuum chamber (not continuously though).

C. Non-reactive versus reactive etching

There are etch parameter ranges, where reproducible meaningful RIE-RAS signals occur. This is an interesting result on its own: etching is not necessarily related to a totally stochastic etch front, but can show certain surface reconstructions, i.e. re-arrangements of the particles on the surface, just like the spectral RAS signal peaks during epitaxy stand for specific (possibly other) surface reconstructions.

The reactive portion of the etch gas should be between 2 and 20 flux-% to warrant reproducible RIE-RAS signals. If the etching is non-reactive or just slightly reactive, etch debris from the chamber wall or from the sample mount will impede the measurement. And if the reactive portion is too strong, the etch process at the etch front will be completely stochastic and typical RAS signals will not occur. Therefore, we use 2 flux-% of chlorine (1 sccm) as the reactive gas in argon as the main plasma gas (50 sccm) in order to get reproducible and meaningful RAS signals. The bias voltage is between 300 and 800 V, the gas pressure in the chamber amounts to $1.3 \cdot 10^{-2}$ hPa. A detailed investigation of influence of the plasma composition can be found in Ref. 10.

Our samples stem from the AlGaAs(Sb) material system on GaAs substrate, but the technique should be useable for dry-etch control of any crystalline semiconductor, probably even of any other crystalline material.

III. RIE-RAS RESULTS

Figure 3 is intended to give an example of a RAS result upon etching of the layer sequence of a AlGaAs(Sb) laser sample with

n- and p-doped layers - (the active layer contains quantum dots, but this is not relevant for the discussion within this contribution) etched with Ar (50 sccm) and Cl₂ (1 sccm). The so-called *RAS color plot* gives the RAS signal in dependence on photon energy $h\nu$ of the RAS light and simultaneously in dependence on elapsed etching time t (here the total process duration has been 33 min). In this case the signal height is color-coded. Red and yellow stand for large positive RAS signal values (maximum at $0.6 \cdot 10^{-3}$ here), green for medium/small ones and blue as well as black for large negative values (minimum at $-1.0 \cdot 10^{-3}$ here). A change of material composition can be monitored by a change in the color-coded RAS spectrum. The data are even sensitive to the doping of the material.

Typically etching is so fast and RAS data collection time is so large (about 0.1 s per value), that only a few (i.e. 11) discrete sampling points (photon energies) per point in etch time can be taken, if a color plot is desired.

Figure 3 also reveals that oscillations of the RAS signal might be observable – especially for small photon energies (large wavelengths). This is due to the fact that the *currently etched* layer constitutes an optical Fabry-Perot resonator/interferometer with continuously *decreasing* thickness. Thus high and low reflectances (anti-resonances & resonances, respectively) will occur periodically.

There are certain conditions for the occurrence of Fabry-Perot oscillations. First of all the materials to be etched should be “transparent enough” at the photon energies of interest to make possible the interferometric superposition of different wave portions going back and forth within the layers. Then the surfaces or interfaces between layers should be smooth enough to warrant Fabry-Perot anti-resonances (large reflectance). But on the other hand non-zero anisotropies at the interfaces are necessary for the occurrence of Fabry-Perot oscillations in the genuine RAS signal. Taking the average reflected intensity instead, Fabry-Perot oscillations can even be expected in the case of no anisotropies at the interfaces.

A. Other techniques

In-situ thickness control is rarely done upon etching (as opposed to growth), but some efforts date back even to about

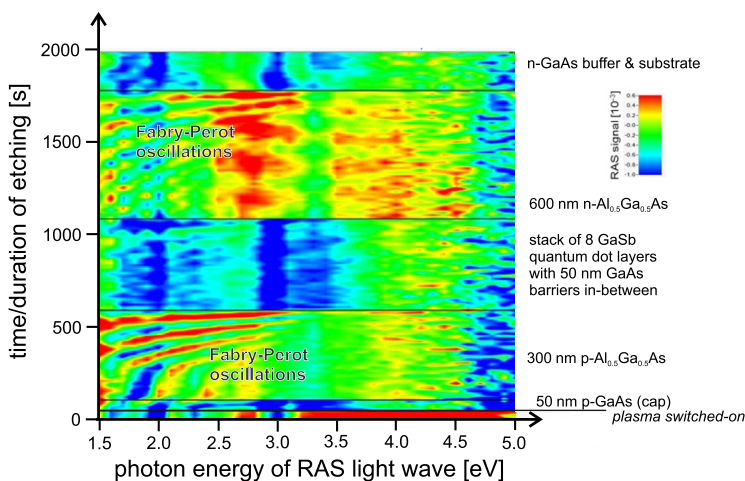


FIG. 3. Example of RIE-RAS result: color plot (signal height color-coded and shown in dependence on time t and photon energy $h\nu$). The range of used photon energies extends from 1.5 to 5.0 eV.

1990.^{14–19} (Interestingly in Ref. 20 the use of RAS for the measurement of morphology changes of a Cu surface in aqueous HCl solution is reported.)

Some of the terms used for those techniques are “reflectance monitoring etching” or “reflectometry ion etching”. In these efforts usually only a single photon energy has been used and Fabry-Perot oscillations, as explained above, are evaluated to retrieve the desired information on etch depth. In most cases of other works, even with broad-band light sources, the light incidence is oblique, yielding ellipsometric information (“spectroscopic ellipsometry”).

In our case^{9–11,21} light incidence is normal to the surface (etch front). Thus typical ellipsometric information is suppressed on purpose and the retrieved information can be connected to orderly oriented anisotropies on a molecular level or to the Fabry-Perot effect.

This contribution is not intended to closely compare RAS results from epitaxial growth with those from etching. Actually one should not expect to have the same surface reconstructions upon etching as in the case of growth, since the sample conditions, especially the substrate temperature, are quite different.

B. Further results & etch depth resolution

The presentation of transients in Fig. 4 is intended to show that not only genuine RAS signals acc. to Eq. (1) might exhibit a significant time evolution, but also the average reflected intensity, which constitutes the denominator in Eq. (1).

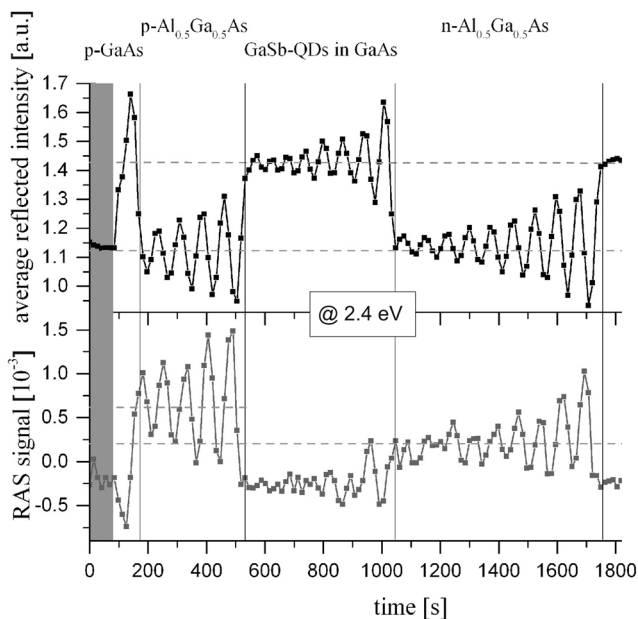


FIG. 4. Transients at 2.4 eV photon energy of the average reflected intensity (top) and of the genuine RAS signal (bottom) during reactive ion etching of another AlGaAs(Sb) semiconductor laser sample with layers of different AlGaAs composition and doping and including GaSb quantum dot layers (the sample is very similar to the one from Fig. 3, but not the same).

The example stems from a wafer which is RIE-etched. Again the layer sequence is that of a semiconductor laser with p- and n-doped AlGaAs(Sb) layers on a GaAs substrate.

The average reflected intensity can even give more pronounced transients than the genuine RAS signal. This is generally the case, when the reflectances/reflectivities of the above-mentioned two wave parts change simultaneously and by similar amounts. In this case the RAS technique is actually not necessary, since the average reflectivity could be measured with simpler equipment. But we consider this an additional opportunity offered by RAS equipment, which we employ also for other reasons (e.g. layer identification). Moreover, it is not clear beforehand, whether the average reflected intensity will reveal oscillations more clearly than the genuine RAS signal.

Obviously the traces in Fig. 4 contain oscillations due to the Fabry-Perot effect. RIE-RAS etch-depth control with an accuracy of 1/4 of an oscillation period should be possible this way, which corresponds to etching further down by $1/(2 \cdot 4) = 1/8$ of the wavelength $\lambda = \lambda_0/n$ inside the material with refractive index n - the factor $1/(2 \cdot)$ since the signal is taken after reflection (the optical path is going forth and back). For a photon energy of 2.4 eV and a refractive index of 4.3, this gives a wavelength of 120 nm inside the material and a resolution of $(120/8) \text{ nm} = 15 \text{ nm}$, an earlier finding by us.²¹ This is a remarkably good value for the accuracy of etch-depth characterization. It becomes even more impressive considering the fact that it has been retrieved *in-situ*, which makes precise etch-depth control feasible.

C. Improving resolution by use of an optical vernier scale

The equivalent of a mechanical Vernier scale in the optical RIE-RAS context (due to the Fabry-Perot resonances it could also be called an interferometric Vernier scale) can be used by employing two different wavelengths or photon energies simultaneously. To the best of our knowledge an interferometric Vernier scale was first mentioned in a patent in 1971.²²

If the photon energies were 10% = 1/10 apart, the achieved accuracy would be $(\lambda/2)/10 = \lambda/20$. And if they were only 5% = 1/20 apart, the accuracy could even be pushed to $(\lambda/2)/20 = \lambda/40$.

Figure 5 gives a RIE-RAS color plot for a dry-etch process of a layer sequence, again of a semiconductor laser (i.e. the one from the measurements underlying Fig. 4).

To illustrate the vernier scale principle we consider the n-doped AlGaAs layer on top of the buffer (etched second to last) here as an example. After a specific etch time (chosen exemplarily and marked with the dashed horizontal red line), for a photon energy of 2.05 eV slightly more than 2 periods (2.xx periods) of the Fabry-Perot oscillations have occurred for this very layer. The “.xx” part has to be deduced.

The idea of any vernier scale is to look for coincidences of the ruler marks of two slightly different scales. In our case of an optical or interferometric Vernier scale the ruler marks are the positions of the Fabry-Perot anti-resonances/maxima in the color plot, taking the reading at two different photon energies/wavelengths for any specific elapsed time.

The Fabry-Perot oscillation period is slightly different for the slightly different wavelengths. The number of the further periods

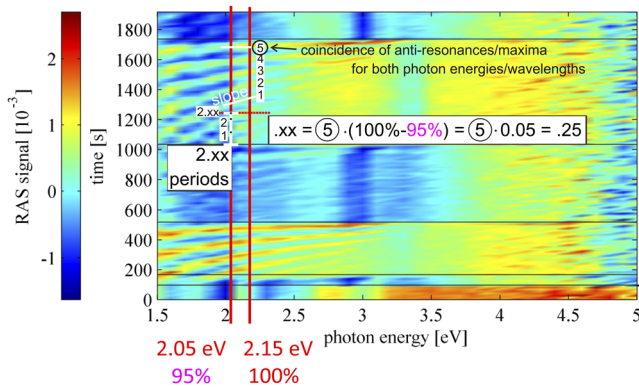


FIG. 5. Color plot of a dry-etch process of a semiconductor laser layer sequence (same sample as the one from Fig. 4). The use of the vernier scale is explained with the help of this figure.

up to the next coincidence of the anti-resonances for the two photon energies/wavelengths reveals the fraction (0.xx) of the oscillation period under investigation.

For the other photon energy 5% apart (i.e. for 2.15 eV) the Fabry-Perot oscillations can also be noticed clearly. The next temporal coincidence of anti-resonances for both wavelengths occurs after 5 additional periods, as marked in Fig. 5. That means that the exact (real) number of periods @ 2.05 eV is

$$2.00 \cdot \frac{\lambda}{2} + 5 \cdot (1 - 0.95) \cdot \frac{\lambda}{2} = [2.00 + 5 \cdot 0.05] \cdot \frac{\lambda}{2} = 2.25 \cdot \frac{\lambda}{2} \quad (2)$$

and “xx” = 0.25 eventually in this example.

For a photon energy of 2.05 eV the vacuum wavelength is 605 nm. Then inside the material with a refractive index of 4.3 the wavelength amounts to 141 nm and the calculated etch depth in this example is

$$2.25 \cdot \frac{\lambda}{2} = 159 \text{ nm} \quad (3)$$

Since a separation of 5% = 1/20 of the photon energies or wavelengths, respectively, has been used, the accuracy of the measurement and the etch-depth resolution are

$$\frac{\lambda}{2} / 20 = 3.5 \text{ nm} \quad (4)$$

Thus the complete result for the etch depth in this example is

$$(159 \pm 3.5) \text{ nm} \quad (5)$$

This result shown an improvement in in-situ etch-depth resolution by more than a factor of 3 as compared to the earlier results mentioned in (B).

Some further remarks have to be made on the optical or interferometric Vernier scale: In the given example the coincidence of the anti-resonances, i.e. the signal maxima, for the two photon energies appears after 5 additional periods of the Fabry-Perot oscillations. What can be done in cases, when the currently etched layer is so thin, that not enough oscillations occur, before a coincidence of anti-resonances/maxima emerges? In order to be able to

computer-calculate on-line the next coincidence it suffices to know the slope of one position function $t(h\nu)$ of the anti-resonances/maxima within the color plot (see again Fig. 5).

But for any layer to be etched away precisely, the corresponding transient should extend over at least one oscillation period, so that the computer can extract the oscillation period safely. In our example this amounts to a minimum layer thickness of $(141/2)$ nm = 71 nm, which is not a strong restriction in most of the III/V semiconductor layer sequences of interest.

The difference in the two considered photon energies accounts for the accuracy of the etch-depth measurement. The smaller the difference, the better is the resolution or accuracy.

IV. CONCLUSIONS

We have successfully employed reflectance anisotropy/difference spectroscopy (RAS/RDS) equipment for in-situ etch depth control during reactive ion etching again.

RAS equipment can be used for etch-depth control, because the layers with etch-related shrinking thickness form optical Fabry-Perot resonators. For a fixed photon energy (wavelength) anti-resonances/maxima of the Fabry-Perot reflectivity occur periodically in time and allow for the extraction of the current etch depth. Our earlier results yielded a resolution of around 15 nm, which should already suffice for most RIE applications. Here we could even improve accuracy further by more than a factor of 3 by use of the measurement data for two similar photon energies. Now the accuracy is improved to values <5 nm, which amounts to about 8 lattice constants - in our examples with AlGaAs(Sb) III/V semiconductor samples. This extremely good in-situ resolution is achievable, because the Fabry-Perot anti-resonances are used as ruler marks in the optical equivalent of a mechanical vernier scale.

ACKNOWLEDGMENTS

This research has been funded by the foundation “Stiftung Rheinland-Pfalz fuer Innovation” under contract 1108 and by the German Research Foundation (Deutsche Forschungsgemeinschaft, DFG) under contracts FO 157/44, FO 157/46, and FO 157/58. Technological assistance by the Nano Structuring Center (NSC) of the Technische Universitaet Kaiserslautern (TUK) is gratefully acknowledged. We also thank Lars Barzen and Ann-Kathrin Kleinschmidt for their earlier work on this subject.

REFERENCES

- ¹D. E. Aspnes, “Above-bandgap optical anisotropies in cubic semi-conductors—A visible near ultraviolet probe of surfaces,” *J. Vac. Sci. and Technol. B* **3**, 1498 (1985).
- ²D. E. Aspnes, J. P. Harbison, A. A. Studna, and L. T. Florez, “Application of reflectance difference spectroscopy to molecular-beam epitaxy growth of GaAs and AlAs,” *J. Vac. Sci. and Technol. A* **6**, 1327 (1988).
- ³J. P. Harbison, D. E. Aspnes, A. A. Studna, and L. T. Florez, “Optical reflectance measurements of transients during molecular-beam epitaxial growth on (001) GaAs,” *J. Vac. Sci. and Technol. B* **6**, 740 (1988).
- ⁴D. E. Aspnes, E. Colas, A. A. Studna, R. Bhat, M. A. Koza, and V. G. Keramidias, “Kinetic limits of monolayer growth on (001) GaAs by organometallic chemical-vapor deposition,” *Phys. Rev. Lett.* **61**, 2782 (1988).

- ⁵N. Esser, M. Kopp, P. Haier, and W. Richter, "Optical characterization of surface electronic and vibrational properties of epitaxial antimony monolayers on III-V (110) surfaces," *Phys. Status Solidi A* **152**, 191 (1995).
- ⁶P. Weightman, D. S. Martin, R. J. Cole, and T. Farrell, "Reflection anisotropy spectroscopy," *Rep. Prog. Phys.* **68**, 1251 (2005).
- ⁷R. Denk, M. Hohage, P. Zeppenfeld, J. Cai, C. A. Pignedoli, H. Söde, R. Fasel, X. Feng, K. Muellen, Sh. Wang, D. Prezzi, A. Ferretti, A. Ruini, E. Molinari, and P. Ruffieux, "Exciton-dominated optical response of ultra-narrow graphene nanoribbons," *Nat. Comm.* **5**, 4253 (2014).
- ⁸G. Bussetti, A. Violante, R. Yivlialin, S. Cirilli, B. Bonanni, P. Chiaradia, C. Goletti, L. Tortora, R. Paolesse, E. Martinelli, A. D'Amico, C. Di Natale, G. Giancane, and L. Valli, "Site-sensitive gas sensing and analyte discrimination in Langmuir-Blodgett porphyrin films," *J. Phys. Chem. C* **115**, 8189-8194 (2011).
- ⁹L. Barzen, J. Richter, H. Fouckhardt, M. Wahl, and M. Kopnarski, "Monitoring of (reactive) ion etching (RIE) with reflectance anisotropy spectroscopy (RAS) equipment," *Appl. Surf. Sci.* **328**, 120 (2015).
- ¹⁰L. Barzen, A.-K. Kleinschmidt, J. Strassner, C. Doering, H. Fouckhardt, W. Bock, M. Wahl, and M. Kopnarski, "Influence of plasma composition on reflectance anisotropy spectra for in situ III-V semiconductor dry-etch monitoring," *Appl. Surf. Sci.* **357**, 530 (2015).
- ¹¹A.-K. Kleinschmidt, L. Barzen, J. Strassner, C. Doering, H. Fouckhardt, W. Bock, M. Wahl, and M. Kopnarski, "Precise in-situ etch depth control of multilayered III-V semiconductor samples with reflectance anisotropy spectroscopy (RAS) equipment," *Beilstein J. Nanotechnol.* **7**, 1783 (2016).
- ¹²N. Esser and W. G. Schmidt, "Atomic structure and optical anisotropy of III-V (001) surfaces," *J. Vac. Sci. Technol. B* **19**, 1756 (2001).
- ¹³A. G. Laytec, Berlin, Germany, www.laytec.de/epiras/.
- ¹⁴T. R. Hayes, P. A. Heimann, V. M. Donnelly, and K. E. Strege, "Maskless laser interferometric monitoring of InP/InGaAsP heterostructure reactive ion etching," *Appl. Phys. Lett.* **57**, 2817 (1990).
- ¹⁵N. J. Ianno, S. Nafis, P. G. Snyder, B. Johs, and J. A. Woollam, "In situ spectroscopic ellipsometry studies of electron cyclotron resonance (ECR) plasma etching of oxides of silicon and GaAs," *Appl. Surf. Sci.* **63**, 17 (1993).
- ¹⁶G. A. Vawter, J. F. Klem, G. R. Hadley, and S. H. Kravitz, "Highly accurate etching of ridge-wave-guide directional-couplers using in situ reflectance monitoring and periodic multilayers," *Appl. Phys. Lett.* **62**, 1 (1993).
- ¹⁷E. Steinsland, T. Finstad, and A. Hanneborg, "Etch rates of (100), (111) and (110) single-crystal silicon in TMAH measured in situ by laser reflectance interferometry," *Sens. Actuators A* **86**, 73 (2000).
- ¹⁸B. S. Stutzman, H. T. Huang, and F. L. Terry, "Two-channel spectroscopic reflectometry for in situ monitoring of blanket and patterned structures during reactive ion etching," *J. Vac. Sci. Technol. B* **18**, 2785 (2000).
- ¹⁹Y. M. Song, K. S. Chang, B. H. Na, J. S. Yu, and Y. T. Lee, "Precise etch-depth control of microlens-integrated intracavity contacted vertical-cavity surface-emitting lasers by in-situ laser reflectometry and reflectivity modeling," *Thin Solid Films* **517**, 5773 (2009).
- ²⁰G. Barati, V. Solokha, K. Wandelt, K. Hingerl, and C. Cobet, "Chloride-induced morphology transformations of the Cu(110) surface in dilute HCl," *Langmuir* **30**, 14486 (2014).
- ²¹C. Doering, A.-K. Kleinschmidt, L. Barzen, J. Strassner, and H. Fouckhardt, "Atomic layer sensitive in-situ plasma etch depth control with reflectance anisotropy spectroscopy (RAS)," *Proc. SPIE* 10329 (2017).
- ²²K. A. Stetson, "Method for measurement of surface profile change using a vernier scale in hologram interferometry," US patent US3612693A (1971).